Microfluidic MEMS

Albert K. Henning
Redwood Microsystems, Inc.
959 Hamilton Avenue
Menlo Park, CA 94025
650-617-0854
henning@redwoodmicro.com

Abstract--The advent of MEMS (micro-electro-mechanical systems) has enabled dramatic changes in diverse technological areas. In terms of control and distribution of liquids and gases (microfluidics), MEMS-based devices offer opportunities to achieve increased performance, and higher levels of functional integration, at lower cost, with decreased size and increased reliability. Microfluidic actuators include distribution microchannels and orifices, microvalves, micropumps, and microcompressors. Related microsensors are required to measure temperature, flow, pressure, viscosity, and density.

This work focuses on the application of microfabricated valves based on the principles of thermopneumatic actuation. A brief comparison to other actuation techniques is made. The science and technology of silicon-based thermopneumatic microvalves is then detailed. The dynamics of the controlled fluid, and thermal and mechanical behavior of structures, necessary to understand the relationships between flow, pressure, and temperature are presented. The power required for actuation, the response speed, and the effect of shrinking size on these parameters are also derived.

In terms of applications, previous research and product development efforts have demonstrated the application of thermopneumatic microvalves to problems of industrial gas and liquid control. Wide ranges of pressure, temperature, and flow rate have been achieved. Expansion valves for refrigeration control have also been produced. Most recently, the integration of microfluidic components using advanced packaging techniques has been used to create devices with higher levels of functionality. Specifically, high-precision pressure regulators, and pressure-based mass flow controllers, have been devised, based upon both normally-open and normally-closed microvalves. Also, low leak-rate shut-off valves, appropriate for use in vacuum system applications, have been developed successfully. At the highest level of integration, these modules have been themselves integrated into mesoscale gas sticks, and gas distribution panels, for use in distribution and control of electronics specialty gases.

List of Symbols and Variables

dV_F, V_o	Volumetric change and initial volume of Fluorinert liquid
β	Temperature coefficient of expansion of Fluorinert liquid
T_{FC}, T_{fill}	Mean and fill temperatures of Fluorinert liquid
s, z, a	Membrane stroke, membrane-to-NO-orifice gap, and membrane radius
h, t	Membrane, cavity thickness
P	Pressure differential across the membrane
E, μ	Young's modulus (190,000 MPa) and Poisson's ratio (0.09) for silicon
σ	Membrane stress
$\dot{m}$	Mass flow (usually in sccm, normalized to 273 K and 1 atm)
P_{in}	Inlet pressure
P_{out}	Outlet pressure
P_x, P_{sense}	Intermediate (pressure sensor) pressure
v, K	Flow velocity, loss coefficient
γ	Ratio of specific heats, c_p/c_v
α	$= \sqrt{\gamma \left(\dfrac{2}{1+\gamma} \right)^{\frac{\gamma+1}{\gamma-1}}}$
δ	$= \sqrt{\dfrac{4\gamma}{(\gamma+1)(\gamma-1)}}$
R	Gas constant in $p = \rho RT$ (8314 m^2/K-sec^2 divided by molecular weight)
ρ	Gas or Fluorinert liquid density
D (or d)	Orifice diameter
A	Orifice area
C_d	Orifice coefficient of discharge
C_{FC}	Fluorinert liquid specific heat capacity
R_{th}	Lumped thermal microvalve resistance

TABLE OF CONTENTS

1. INTRODUCTION

Microfabrication techniques created for the semiconductor integrated circuit industry have found new applications in MEMS research, development, and manufacture. To a certain degree, the name 'MEMS' is a misnomer, since it encompasses not simply devices employing electrical and mechanical phenomena; but chemical, thermal, fluidic, biological, and optical mechanisms, as well. In this work, we focus on MEMS in the context of fluidics.

Microfluidic MEMS are comprised of a variety of components. *Sensors* are used to measure fluid properties such as pressure, temperature, and flow. Capacitance and pizeoresistance are the usual means to measure pressure. Thermocouples, precision resistors, and *pn* junction diodes are used to determine temperature. Flow is measured using thermal means (monitoring the transit time of a thermal pulse imparted to the fluid), vortex generation, or by monitoring the pressure across an orifice. **Actuators** such as pumps, compressors, and valves are used to alter the state of the fluid pressure, temperature, or flow. Actuators rely on a variety of activation mechanisms, such as electromagnetic, electrostatic, pneumatic, bimetallic alloys, shape-memory alloys (SMA), electrochemical, and thermopneumatic. *Distribution channels*, such as orifices and microchannels, carry the fluid from one portion of the system to another.

A crucial, and often underappreciated, aspect of MEMS is the requirement for **systems integration** of microfabricated components. Electronics, control algorithms, materials compatibility in the fluidic wetted path, packaging, and system testing are critical to the achievement of a robust and fully functional system. Fabricating only the micro-components of the system is never sufficient.

Microfluidics **applications** abound in the automotive, refrigeration and home appliance, control, medical and biomedical, aeronautical, and industrial process arenas.

Microvalves are a primary component of microfluidic systems. As such, they offer a vehicle to compare and contrast different actuation mechanisms. The major bases for comparison are closing force (*pressure range* of operation), *temperature range*, *speed*, and *reliability*. The actuation principle employed in our work has been based on the thermopneumatic deflection of a thin silicon membrane [1]. Other valve actuation methods have been explored [2, 3]. Thermopneumatic actuation relies on the change in volume of a sealed liquid or solid, under thermal loading, to move a membrane against a valve seat. The mechanical work 'stored' in a liquid or solid which can be expanded exceeds the energy stored in an electromagnetic or electrostatic field – giving thermopneumatic actuation a closing force advantage. *Pressure ranges* from vacuum up to at least 200 psia have been demonstrated. In terms of *temperature range*, pure pneumatic actuation offers the widest range of operation, since an applied pneumatic pressure deflect a membrane, regardless of the thermal state of the system. For each of the other actuation techniques, however, temperature imposes restrictions. Membranes in electromagnetic, electrostatic, bimetallic, and SMA microvalves tend to be polycrystalline or amorphous. As a consequence, temperature affects the stress in these thin film materials, so that the range of temperature can be limited. In electrochemical microvalves [4], since chemical reactions are driven thermally, ambient temperature can have a strong effect on response times. For thermopneumatic valves, the choice of the structural parameters, and the choice of the thermopneumatic liquid, can either limit or extend the range of temperature operation. In the best instance, the range can be as wide as -20 °C to 70 °C, if the fluid flow surface (with high heat transfer) is isolated thermally from the heat input [5].

In terms of *speed*, any thermally-based actuation process will be slow in comparison to electrostatic or electromagnetic mechanisms, and when compared to SMA means. Very simply, the product of electrical resistance and capacitance for a material tends to be less than its thermal counterpart. So, electrostatic actuation with 1 μsec response time has been shown, while thermopneumatic response times at present valve sizes are 40 msec or slower. However, as will be shown, thermopneumatic actuation still offers relatively high speeds as devices scale downward in size. The use of single crystal silicon means thermopneumatic microvalves do not suffer from the 'work hardening' which occurs in bimetallic alloys, or in shape memory alloys, and which leads to long-term *reliability* difficulties.

In the remainder of this work, the principles of thermopneumatic microvalve technology will be described first. Applications to the control of refrigerant liquids will be described briefly. A detailed discussion concerning applications to semiconductor processing, and conclusions, complete the work.

2. THERMOPNEUMATIC MICROVALVE TECHNOLOGY

The development of thermopneumatic microvalves requires an understanding of the fluidic, mechanical, and thermal behavior of overall structure.

An example microvalve cross-section is shown in Figure 1. Only a single valve is shown, though hundreds of such devices are created using wafer-scale fabrication techniques. The fabrication sequence is shown in Figure 2. This device is a normally-open (NO) microvalve. That is, with no electrical input, it facilitates full flow. The valve behaves in the following fashion. When electrical current is forced through the Pt resistor, the resistor heats up. This heat is then transferred to the Fluorinert™ (FC) liquid in the hermetically sealed, thermopneumatic cavity. The

472

liquid expands upon heating. Since the cavity is mechanically rigid on all sides except the silicon membrane side, the membrane deforms or deflects in response to the thermal expansion of the liquid, and either modulates flow, or closes off flow entirely.

Fluidic Design

The flow through the unpowered valve is the first parameter which must be determined. The discussion here will focus on gas, and not liquid, flow. If there is no viscous loss, then the compressible flow in the subsonic regime can be expressed as [6]:

$$\dot{m} = \frac{P_{in}}{\sqrt{RT}} C_d A \left(\frac{P_{out}}{P_{in}}\right)^{1/\gamma} \delta(\gamma) \sqrt{\left(\frac{P_{in}}{P_{out}}\right)^{\frac{\gamma-1}{\gamma}} - 1} \quad (1)$$

Sonic flow can be expressed as:

$$\dot{m} = P_{in} C_d A \frac{\alpha(\gamma)}{\sqrt{RT}} \quad (2)$$

Flow in the microvalve itself rarely, however, enters the sonic regime. In fact, for pressure drops more than approximately 5 psid through the valve, viscous losses become important, and a loss-coefficient model must be used to characterize the flow. For normally-open valves, where the flow through an inlet impinges on the valve membrane, an alternative approach is to describe the flow in terms of a loss coefficient K, defined as $K \equiv \Delta P / \left(\rho_{in} v^2 / 2\right)$. If the mass flux is expressed as $\dot{m} = \rho A v$, then the flow (regardless of sonic or subsonic regime) can be expressed as:

$$\dot{m} = A \sqrt{\frac{2}{K} \rho_{in} \left(P_{in} - P_{out}\right)} \quad (3)$$

In this instance, the expression for our measured loss coefficients, for impingement flow, is:

$$K = 24123 \cdot \exp\left(-\frac{z/d}{0.027}\right) + 5854 \cdot \exp\left(-\frac{z/d}{0.546}\right) \quad (4)$$

where z is the distance between the valve membrane and the valve inlet orifice at full-open flow, and d is the hydraulic diameter of the valve inlet. These measurements of impingement flow through a silicon orifice of 570 μm have shown the best control range for the microvalve occurs when the ratio of maximum membrane deflection z to orifice diameter d is less than 0.2, as shown in Figure 3.

Mechanical Design

As mentioned, the thermopneumatic actuation principle relies on a hermetically sealed cavity, which is filled with FC liquid. The valve membrane moves in response to thermal expansion of this liquid, and ultimately forms a seal with the valve seat, which is also comprised of silicon.

Figure 4 shows a schematic representation of the membrane deformation, related to the variables in the following equations. The behavior of the NO device is described in [1]. Additional descriptions for the behavior

of single-crystal silicon membranes may be found in [7]. In terms of the device behavior, the following equations provide the most immediate insight. Equation (5) describes the change in volume in the sealed cavity, as a function of the coefficient of thermal expansion of the FC liquid, fill temperature of the liquid, and mean temperature of the liquid:

$$dV_F = V_0 * \beta * (T_{FC} - T_{fill}) \quad (5)$$

The change in cavity volume is also related to the geometrical shape of the membrane as it deforms. If the membrane is assumed to be spherical:

$$dV_F = \frac{1}{6}\pi s(3a^2 + s^2) \quad (6)$$

These expressions create a relationship between the membrane stroke s (the departure from its equilibrium position z), and the power input to the valve as defined by the mean FC temperature T.

The stroke s may also be considered as a response to P, the transmembrane pressure:

$$s = 0.0151 \cdot (1 - \mu^2) \cdot \frac{Pa^4}{Eh^3} \quad (7)$$

Simultaneously, the deformation of the membrane creates stress in the silicon:

$$s = 0.0491 \cdot (1 - \mu^2) \cdot \sigma \cdot \frac{a^2}{Eh} \quad (8)$$

From a design perspective, then, an NO valve must meet the ambient temperature specifications, while closing against the specified system pressures, while minimizing the power consumption, and staying well below the fracture strength of the crystalline silicon.

Thermal Design

The thermopneumatic microvalve is, in one sense, a complicated device. It involves a hermetically sealed fluid, while modulating the flow of the fluid being controlled. It combines three-dimensional mechanical and thermal behavior. The fluid flow further complicates the picture, since it provides a convective mode for heat transfer from the device, beyond the obvious conductive mode.

However, physical understanding of the device behavior can be obtained from a one-dimensional model. The time-dependent heat transfer equation (balancing heat stored, with the difference between heat input, and heat output, per unit time) is:

$$\rho V_0 C_{FC} \frac{dT_{FC}}{dt} = P_{in} - \frac{T_{FC} - T_{ambient}}{R_{th}} \quad (8)$$

Under steady-state conditions, the mean temperature of the FC liquid is seen to be related linearly to the input power, the lumped thermal resistance between the FC liquid and the ambient, and the ambient temperature:

$$T_{FC,ss} = P_{in} R_{th} + T_{ambient} \quad (9)$$

Continuing with the discussion of Equation (8), if we look at the full transient behavior of the valve in going from an unpowered to a powered state, then the time associated with deflecting the membrane an amount s (assuming all the energy input goes into the FC liquid, and is not lost to the surroundings) is:

$$t_{rise,min} = \frac{\rho C_{FC}}{\beta} \frac{1}{P_{in}} \frac{1}{6} \pi s(3a^2 + s^2) \qquad (10)$$

The rise time thus is related to the material parameters of the FC liquid, inversely proportional to the rate at which heat is input, and proportional to the deflection of the membrane. Using Equation (10), the effect of scaling microvalve size can be explored. Figure 5 shows the results of scaling on the rise time, leading to the expectation that millisecond timescales are achievable for relatively small, but realizable, microvalve devices.

Using alternative heat transfer methods in the FC liquid cavity (for instance, utilizing a liquid-to-gas phase transition to obtain faster volumetric changes [8]), a ten-to-twenty fold reduction in these response times can be obtained.

3. REFRIGERATION APPLICATIONS

Normally-open microvalves have been applied to the problem of controlling liquid flow. In particular, water and R-134a (an approved, new refrigerant liquid) have been controlled successfully [5]. Flow rates consistent with refrigerant requirements for small commercial air conditioners (~10 gm/sec) have been demonstrated. Figure 6 shows the pressure vs. flow vs. valve power input for one such microvalve.

Refrigerant liquids present unusual challenges for thermally activated microvalves. Since the refrigerant's thermodynamic state is being carefully prepared, to be on the edge of flashing just after the valve, and just prior to entering the system evaporator, the valve itself must impart little or no heat to the refrigerant liquid. In this instance, we modified the valve structure shown in Figure 1, adding a second, hollow Pyrex layer between the capping Pyrex layer and the membrane layer. This hollowed layer, filled with FC liquid, served to isolate the membrane thermally from the heater resistor (since the FC liquid has the lowest thermal conductivity in the microvalve), allowing little heat to be removed from the microvalve by the refrigerant.

4. SEMICONDUCTOR PROCESS APPLICATIONS

The present and future requirements of the semiconductor industry for gas distribution and control are well documented [9,10]. The arrival of facilities to fabricate 300 mm silicon wafers creates opportunities for new technologies to meet the challenging performance, cost, yield, and reliability specifications for devices manufactured in these facilities. The gas control and distribution portions of these facilities will be faced with particular challenges. Particles must be reduced in size and number. This reduction requires: increased materials compatibility with process gases; decreased dead space volumes; decreased numbers of, or improved welds; and decreased numbers of, or improved, face seals.

Several conventional means to meet these challenges have been proposed [11]. Approaches based on MEMS offer numerous advantages. Materials in silicon-based microvalves and microfluidic systems are compatible with a wide range of electronics specialty gases (ESG). Where the gas in question is corrosive to silicon, thin film coatings such as SiC and Si_3N_4 may be used to coat the wetted surfaces and restore corrosion resistance [12]. Decreased dead volumes have already been demonstrated in micro-chemical analysis systems [13]. Laboratory versions of MEMS-based electrostatic microvalves have been reported [4].

In order to create a true system, MEMS-based devices require a number of components. The components utilized in our gas control and distribution devices include: the underlying flow model (supported by the electronics); critical flow orifices; normally-open proportional valves; normally-closed shut-off valves; temperature and pressure sensors; and the advanced ceramic packages which combine the modules into higher-level devices.

Using these components, we have created several modules to address the needs of semiconductor processing. Vacuum leak-rate shut-off valves; low-flow, high-precision mass-flow controllers (MFCs); and pressure regulators have been achieved. We have also developed ultraclean packaging technology, which allows these modules to be incorporated into compact gas panels.

Each shut-off valve module includes a normally-closed microvalve with an elastomeric seal incorporated with the silicon micromachined structure. Each MFC and pressure regulator contains a temperature sensor, an E^2PROM (which contains the gas- and temperature-dependent calibration information for the unit) and one or two pressure sensors. In addition, the MFC also includes a critical-flow orifice, to execute the pressure-based flow control algorithms we have employed.

Vacuum Leak-Rate Shut-off Modules

Normally-closed (NC) valves are important components of other MEMS-based microvalve devices [14]. We have created NC valve modules which have a wetted path composed entirely of ceramic (Al_2O_3) or silicon. These valves also have incorporated a proprietary sealing technology, which enables very low leak rates to be obtained [15]. As with the NO valve (MFC or pressure

regulator) modules, wetted surfaces may be coated with SiC or Si_3N_4, in order to provide materials compatibility in situations where a wetted silicon surface would be undesirable.

Figure 7 shows a cross-section of this normally-closed, low-leakage shut-off valve. The thermopneumatic actuation principle is still employed. In this case, however, a boss is added to the silicon membrane, and a silicon cantilever is either fusion-bonded to the boss. Under conditions of zero input power, this cantilever will provide the shut-off property by sealing against a low-leakage seat (polished silicon). As shown, the wetted path is entirely silicon or ESG-compatible ceramic. The silicon-ceramic interface is a eutectic bond. The overall dimensions are 8 mm x 6 mm x 2 mm, and are (roughly) to scale.

Figure 8 shows the schematic cross-section of the sealing interface between an elastomer (o-ring) and the polished silicon valve seat. The sealing force compresses the elastomer, as depicted. Approximately, the leak rate through the elastomer, as a function of pressure drop, gas diffusion coefficient for the elastomer, and o-ring geometry, is:

$$\dot{m}_{leak} \equiv 2\pi R \cdot \Delta P \cdot k \cdot 2 \int_0^{y_{max}} \frac{dy}{2\sqrt{r^2 - y^2}} \qquad (11)$$

Our calculations based on Equation (11) encouraged the design and fabrication of the vacuum leak-rate NC valves. Figure 9 shows measured helium leak rates for a set of such devices. The sealing material in these devices is Viton; we are in the process of characterizing seals made with other materials, such as Kel-F™. Also shown is data from a standard shut-off valve commonly used in the industry. The SEMATECH specification for shut-off valves is less than 10^{-9} cc-He/sec after 15 seconds of shut-off. Shut-off valves used at present in the industry reach higher steady-state leak rates than these microvalves, due to their more permeable sealing materials, or smaller compression forces on the sealing surfaces. At the same time, the width of their sealing surfaces is greater than in our microvalve, occasionally resulting in lower metastable values of leak rate.

High-Precision Mass-Flow Controller and Pressure Regulator

The specifications for a high-precision MFC are shown in Table I. Of particular importance are the specifications for resolution and repeatability. Controlling etch and deposition process chemistries for the semiconductor industry demand

The design of gas control devices begins with the models for flow given in Equations (1-4). The MFC device is shown in cross-section in Figure 10. The pressure regulator has the same configuration, but without the critical orifice. The MFC operates using the linear relationship between sonic (critical) flow through an orifice

[Equation (2)], and the pressure upstream of the orifice [6]. To ensure critical flow, the pressure upstream of the orifice must exceed the downstream pressure by roughly a factor of 2 (this factor is gas-dependent [6]).

Table I: Specification for low flow MFC.

Fluid Media:	Corrosive Gases and Liquids
Maximum Flow Rates:	1, 10 sccm (N2 at 20 psid)
Turndown Ratio:	5:1
Accuracy:	± 1% of F.S.
Repeatability:	± 0.5% of F.S.
Resolution:	± 0.1% of F.S.
Response Time:	500 ms typical
Valve Leak Rate:	5 x 10^6 cc/sec He
Inlet Pressure Range:	0 to 50 psig
Maximum Outlet Pressure:	10 Torr
Temperature Range:	0 to 50°C
Power Consumption:	2.0 W typical
Dimensions:	106 mm x 40 mm x 25 mm

Figure 10 shows a schematic of the mass flow measurement principle. The control electronics manage the relationship between pressure and temperature sensors, and power input to the various valves in the flow control and distribution devices. Pressure and temperature sensors near the critical orifice are used with Equation (2) to extract the mass flow rate. Depending upon the mass flow set point for the device, the electronics provide the feedback control to the normally-open proportional valve, in order to match the flow rate with the set point, within the accuracy and resolution specifications.

Critical Flow Orifices for MFC Modules

The critical orifices (COs) used in our MFC modules are fabricated using silicon conventional, wet anisotropic etching to create the sharp, beveled orifices required for Equation (2) to hold.

Using Equation (2), the area and coefficient of discharge of the critical orifice, and the gas type, set the maximum specified flow rate for the MFC. The output pressure specification then sets the dynamic range of the MFC, since it limits the output pressure for the CO, and so limits the upstream pressure range for which the flow through the CO will satisfy Equation (2).

MFC modules may be used with a wide variety of gases, without re-calibration, since the gas-dependent parameters required to extract flow information from the measured pressure upstream of the CO are stored in the module's E^2PROM.

Resolution is closely tied to the size of the critical orifice. Figure 11 shows the nature of this relationship. The results assume He flow associated with a low-flow MFC. The inlet and outlet pressures are assumed to be 30 psia and 100 Torr, respectively. The pressure sensor electronics

are assumed to have 12 bits of analog to digital conversion in the sensing path, of which 2 bits may be 'lost' to noise. The flow model of Equation (2) is assumed. For example, if a 0.01 sccm He flow resolution is desired, and the minimum pressure resolution is 0.03 psia, then the critical orifice's linear dimension must be less than 20 μm.

Principles of Operation

Using the flow models shown earlier [Equations (1-4)], it is possible to model the behavior of the low-flow MFC. A series combination of a CO and NO is the simplest device-level flow model, as shown in Figure 12. Assuming the isentropic flow (no viscous energy loss) model of Equation (1), the NO orifice area is, in effect, set by of the walls of a cylindrical tube:

$$A_{NO} = \pi D_{NO}(z - s) \qquad (12)$$

As the power to the NO valve is increased, this effective area decreases, and the flow decreases. P_X represents the pressure to be sensed by the pressure sensor, which will be fed back into the electronics in order to control the NO valve. The flow model of Equation (3) incorporates z directly includes nonisentropic energy losses.

Figures 13-16 show measurements from a completed MFC. Most of the specifications in Table I have been met by these early MFC modules. Power consumption for the 1 and 10 sccm units are less than 0.5 W. Further improvements are expected in subsequent iterations of the

In Figure 17, the intersection of the NO and CO flow curves determines the value of the pressure P_x, as a function of the membrane-to-inlet gap z-s. Using Equation 2, this pressure also determines the mass flow. When the NO valve is unpowered, the membrane-to-inlet gap is the full value z, and very little pressure is dropped across the NO valve. As s increases, more pressure is dropped across the NO, and the flow decreases. Power input to the NO valve, (related inversely to the signal voltage applied in Figure 13) is responsible for increasing s (see Equations 5-6), and decreasing the membrane-to-inlet gap. The conditions for Figure 17 are: N_2 flow; $A_{CO}=(16.5)^2$ μm²; z-s=2 μm; D_{NO}=25 μm.

Control of the mass flow is effected by comparing the flow determined from the pressure sensor measurement, and comparing it to a set point.

If the flow is too high compared to the set point, additional power is sent to the NO valve, increasing s, and decreasing the MFC flow. If the flow is too low, the power input to the NO valve is decreased, causing s to decrease back toward the unpowered value z. Temperature-dependent information, compensating for temperature-induced package stresses on the pressure sensor, and temperature-related changes in flow in Equation 2, are stored in an E²PROM on the MFC module (see Figure 18).

	# of Welds	# of Seals	Internal Volume
1990	10	0	38 cc
1995	6	8	31 cc
1996	3	12	22 cc
1997	0	10	2 cc
1998	0	0	<1 cc

Table II: Functional comparison of present and future integrated gas sticks/panels (after [11]).

Sensors (Pressure, Temperature)

In our present devices, small (several millimeters square) temperature sensors and piezoresistive pressure sensors are used to monitor temperature and pressure in the device flow path. These sensors are commercially available. When incorporated into a final flow control device, the information they provide becomes the basis for the temperature and pressure calibration data which is stored on E²PROM. It is important that sensing occur as close as possible to the flow point of interest. For instance, in a low-flow MFC, the pressure must be sensed as close as possible to the inlet of the critical orifice.

Advanced Ceramic Packaging

Ceramics available as a result of advances in semiconductor integrated circuits have the structural and materials properties required for application to ESG delivery and control. Figure 18 extends the cross-section of, for instance, Figure 10, and shows an isometric view of the use of such ceramics for pressure regulation, mass flow control, or low-leakage shut-off applications. The ceramics allow integration of an E²PROM, which holds the calibration constants for the particular device, as well as constants for a variety of gases. A metal lid provides a hermetic seal for the valve modules, and the pressure and temperature sensing modules. Electronic control signals are communicated via metal lines patterned on the ceramic surface.

Gas Distribution Devices

MEMS-based modules can be combined to create a hierarchy of gas control and distribution devices. Some of these devices, such as the pressure regulator or the MFC, can themselves be used to build still higher levels of functionality, in the form of, for instance, a fully integrated, multiple-channel gas panel.

Figure 19 shows schematic and isometric views of a fully-integrated gas panel, comprised of four single-channel gas sticks. The manifold on which the individual modules reside is typically built from stainless steel. The size of this gas panel compares very favorably to existing designs. As shown in Figure 20 and Table II, existing panels with

identical functionality occupy ten times the area of 1995 panel designs, and over four times the area of 1996 designs.

5. CONCLUSIONS

We have demonstrated the science and technology required to design and fabricate flow distribution and control devices suitable for the semiconductor processing industry. Components such as pressure-based flow models, critical orifices, pressure and temperature sensors, normally-open proportional valves, and normally-closed vacuum leak rate shut-off valves, have developed. The valve actuation is based on previously developed thermopneumatic techniques. These components have been integrated into shut-off valve, mass flow controller, and pressure regulator modules, which themselves are combined at a higher level into integrated gas panels. Each integrated device has the benefit of small size, lower cost, higher resolution, materials compatibility, and lowered defect generation, which are among the attributes of the successful application of MEMS-based technology.

6. ACKNOWLEDGMENTS

7. REFERENCES

[1] M. J. Zdeblick and J. B. Angell, In Proceedings, *Transducers '86 (1986 Int'l. Conf. Sol. State Sens. and Act.)*, pp. 827-829 [IEEE, Piscataway, NJ, 1986]; M. Zdeblick, "A planar process for an electric-to-fluidic valve." Ph.D. dissertation, Stanford University, June, 1988; and, M. Zdeblick, "Integrated, microminiature electric-to-fluidic valve and pressure/flow regulator." U.S. Patent 4,821,997 (1989).

[2] P. W. Barth, "Silicon microvalves for gas flow control." In Proceedings, *Transducers '95 (1995 Int'l. Conf. Sol. State Sens. and Act.)*, pp. 276-279 [IEEE, Piscataway, NJ, 1995]; and references therein.

[3] J. Robertson, "An electrostatically-actuated integrated microflow controller." Ph.D. dissertation, U. Michigan, 1996.

[4] D. Hopkins, "Electrochemical actuator, and method of making same." U.S. Patent 5,671,905 (1997).

[5] A. K. Henning, et al., "A thermopneumatically actuated microvalve for liquid expansion and proportional control." In Proceedings, *Transducers '97 (1997 Int'l. Conf. Sol. State Sens. and Act.)*, pp. 825-828 [IEEE, Piscataway, NJ, 1997]

[6] Frank M. White, Fluid Mechanics. McGraw-Hill (New York, 1979)

[7] Mario di Giovanni, Flat and Corrugated Diaphragm Design Handbook. Marcel Dekker (New York, 1982)

[8] A Cooperative Research and Development Agreement between Redwood Microsystems and Lawrence Livermore National Lab led to this finding. Patent application in progress.

[9] The National Technology Roadmap for Semiconductors. 1994 (Semiconductor Industry Association, San Jose, CA)

[10] See, for instance, papers presented in the "Manufacturing Science and Technology Technical Group" sessions of the 43rd National Symposium of the American Vacuum Society, Philadelphia, PA, October 14-18, 1996.

[11] J. Cestari, D. Laureta, and H. Itafuji, "The next step in process gas delivery: a fully integrated system." *Semiconductor International*, January 1997, pp. 79-87.

[12] A. F. Flannery, et al., "PECVD silicon carbide for micromachined transducers." In Proceedings, *Transducers '97 (1997 Int'l. Conf. Sol. State Sens. and Act.)*, pp. 217-221 [IEEE, Piscataway, NJ, 1991]

[13] S. Shoji, B. Van der Schoot, N. de Rooij, and M. Esashi, "Smallest dead volume microvalves for integrated chemical analyzing systems." In Proceedings, *Transducers '91 (1991 Int'l. Conf. Sol. State Sens. and Act.)*, pp. 1052-5 [IEEE Press, Piscataway, NJ, 1991]

[14] See the Fluistor™ product literature and specifications from Redwood Microsystems (e.g., http://www.redwoodmicro.com).

[15] Patent applications in process.

8. BIOGRAPHY

Albert K. Henning was born in 1955. He received the A.B. (magna cum laude) and A.M. degrees from Dartmouth College in Physics in 1977 and 1979, respectively. He worked as a device physicist with Intel Corporation from 1979 to 1982. He completed his Ph.D. (EE) at Stanford University in 1987. From 1987 to 1995, he was Assistant, and then Associate, Professor of Engineering Science at the Thayer School of Engineering, Dartmouth College, where he designed, built, and equipped a Class 100/1000 clean room facility for microelectronics and microstructures teaching and research. He spent portions of the 1993-94 academic year on sabbatical, as a Visiting Scientist in the Microstructures Technology Laboratory at

MIT. In 1996 he joined Redwood Microsystems, where he presently serves as a member of the Executive Staff, as a Program Manager for research, development, and productization for several microfluidic devices, as Principal Investigator for several Federally-funded research projects, and as Wafer Engineering Manager. His research interests over the years include: low temperature behavior of semiconductor and MOSFET devices; high-field transport modeling in MOSFETs; SiGe MOSFETs fabrication and modeling; and especially development of scanning probe microscopy for dopant profiling, technology characterization and failure analysis in MOSFETs. Most recently, he has worked on micromachining process technology and MEMS device development, ranging from: thermocouple MOSFETs and arrays; biomagnetic sensors; and especially microfluidic devices and technology, including stress-engineered microstructures, microturbines, micronozzles, microvalves, and the microvalve-based devices as described herein.

He received an Analog Devices Career Development Professorship in 1987, and an IBM Faculty Development Award in 1990. He holds one U.S. Patent (on the thermocouple MOSFET), and has four other applications in progress. He has published over fifty articles in archival proceedings and journals. He is a member of Sigma Xi, ASEE, and IEEE.
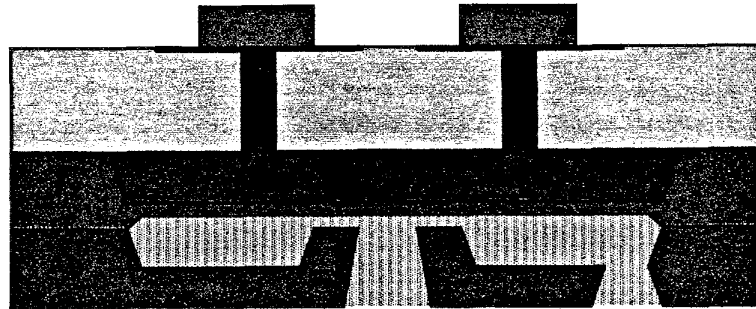
Figure 1: Cross-Section of a Thermopneumatically-Actuated, Normally-Open, Proportional Microvalve. The Inlet (center hole) is the Smallest of the Two Holes.

Step 1: Drill holes in Pyrex wafer ultrasonically

Step 2: Metallize Pyrex wafer

Step 3: Define membrane wafer lithographically (gold, oxide, photoresist masks)

Step 4: Etch membrane wafer in KOH; strip masking materials

Step 5: Define orifice wafer lithographically (gold, oxide, photoresist masks)

Step 6: Etch orifice wafer in KOH; strip masking materials

Final Steps: Fusion bond membrane andorifice wafers; bond Pyrex to this sandwich anodically; fill thermopneumatic cavity with liquid; seal with silicon caps.

Figure 2: Fabrication Sequence for a Normally-Open, Thermopneumatic Microvalve.
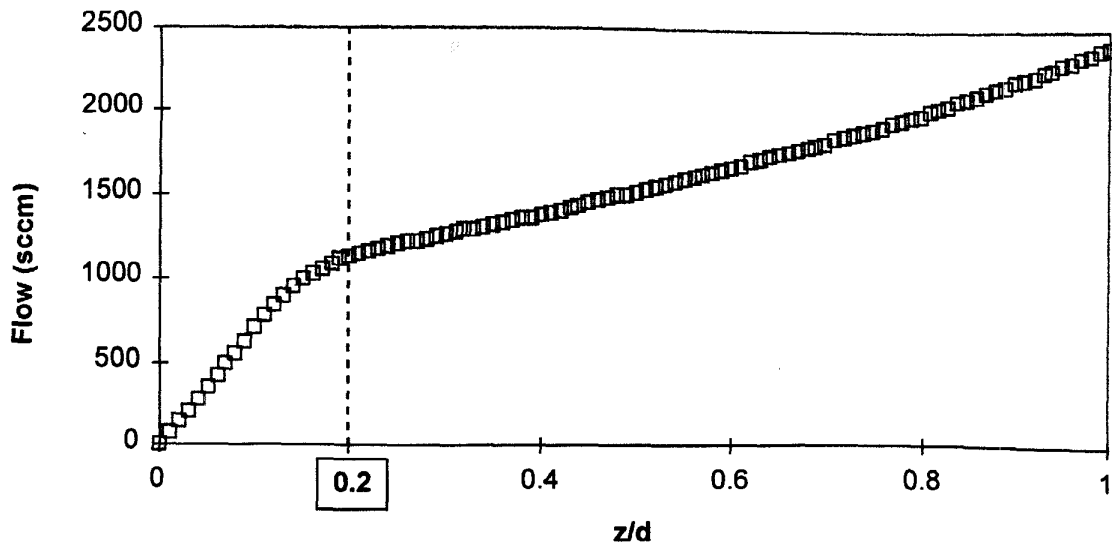
Figure 3: Estimated Flow Based on Loss Coefficient Flow Measurements: N_2, P_{in}=16 psia, P_{out}=14.7 psia, d=570 μm, T=300 K.
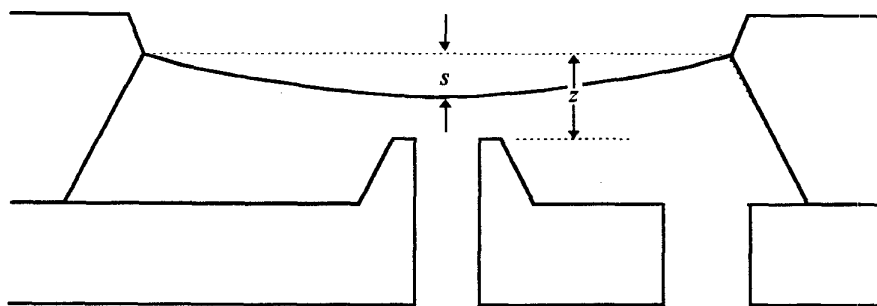
Figure 4: Relationship between the Equilibrium Membrane-to-Inlet Distance z and the Stroke s.
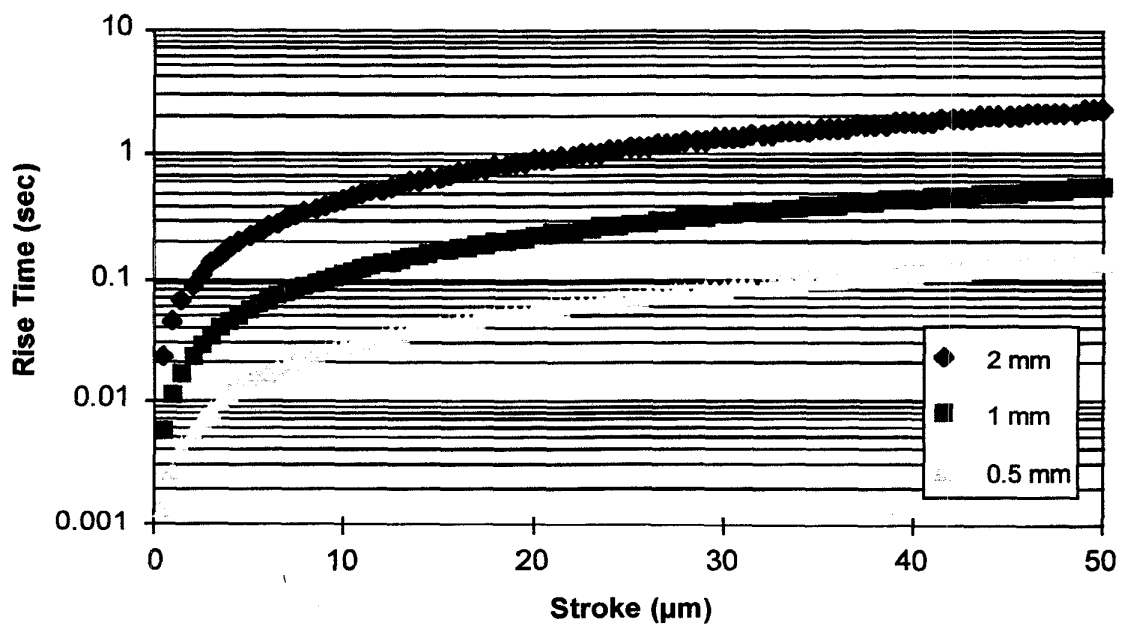
Figure 5: Predicted Effect of Scaling on Microvalve Response Time.
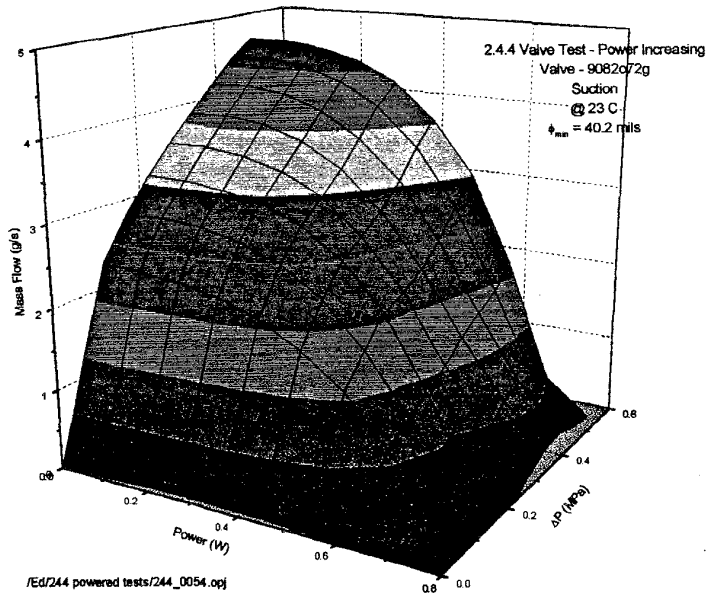
Figure 6: Pressure vs. R-134a Flow vs. Power for a Representative Microvalve.

Outlet   **Inlet**
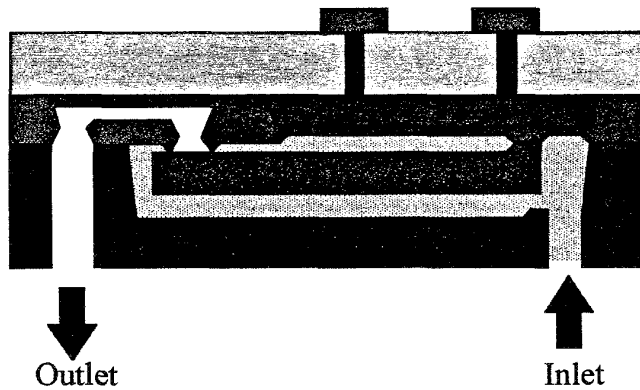
Figure 7: Cross-Section of a Thermopneumatically-Actuated, Normally-Closed, Low-Leakage Shut-Off Valve.

Compression

$y = y_{\max}$

$y = 0$

Sealing Force
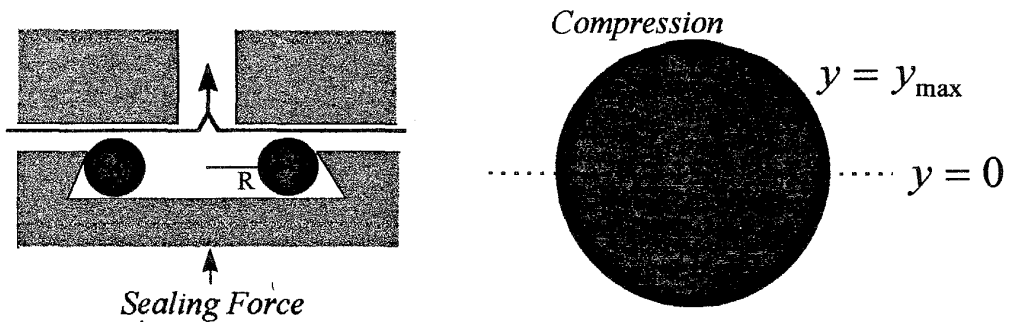
Figure 8: Schematic of O-ring Used in the Vacuum Leak-Rate Shut-Off Module/Valve.
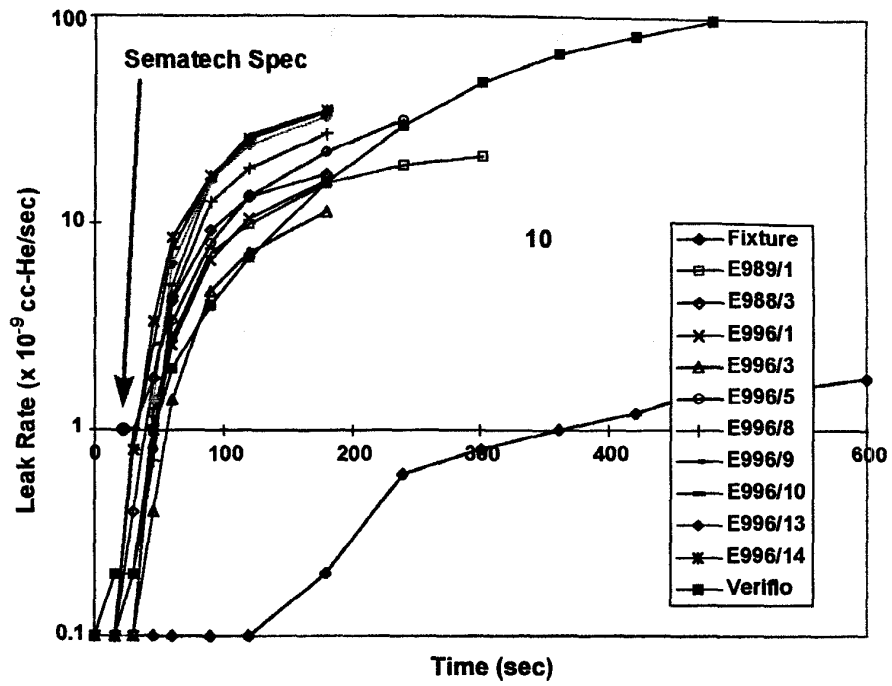
Figure 9: Helium Leak Rate for Vacuum Leak-Rate Shut-Off Microvalves.
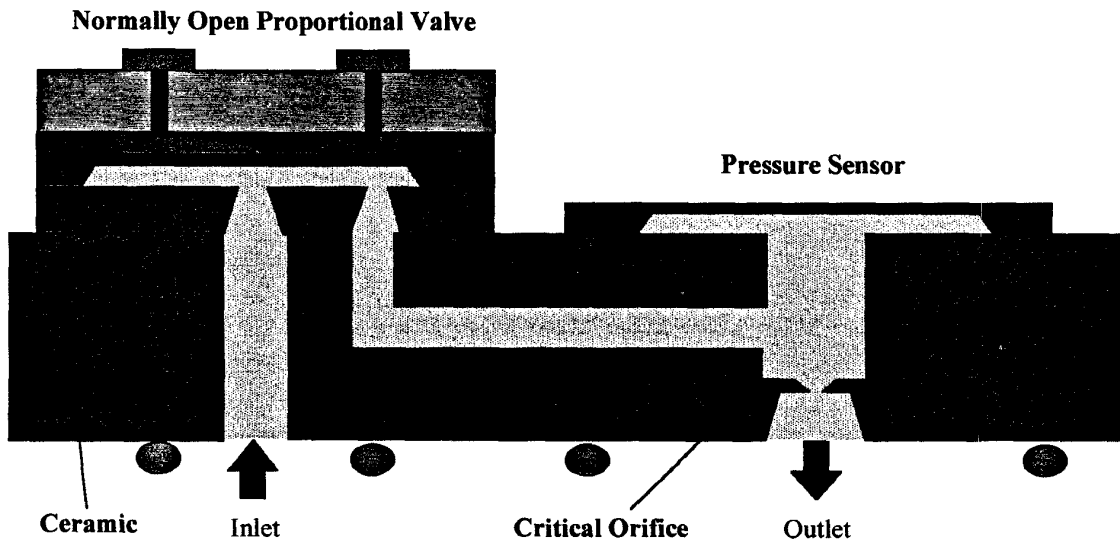
Figure 10: Schematic Representation of the Low-Flow MFC.

1000

Appropriate Orifices

Pressure Resolution (psi)

0.001　　　　　0.01　　　　　0.1　　　　1

100

10

1

0.1

0.01

Flow Resolution (sccm)

0.001

◆	2 μm
■	3 μm
▲	4 μm
✕	5 μm
✻	6 μm
●	7 μm
+	8 μm
—	9 μm
—	10 μm
◆	12 μm
■	15 μm
▲	20 μm
✕	25 μm
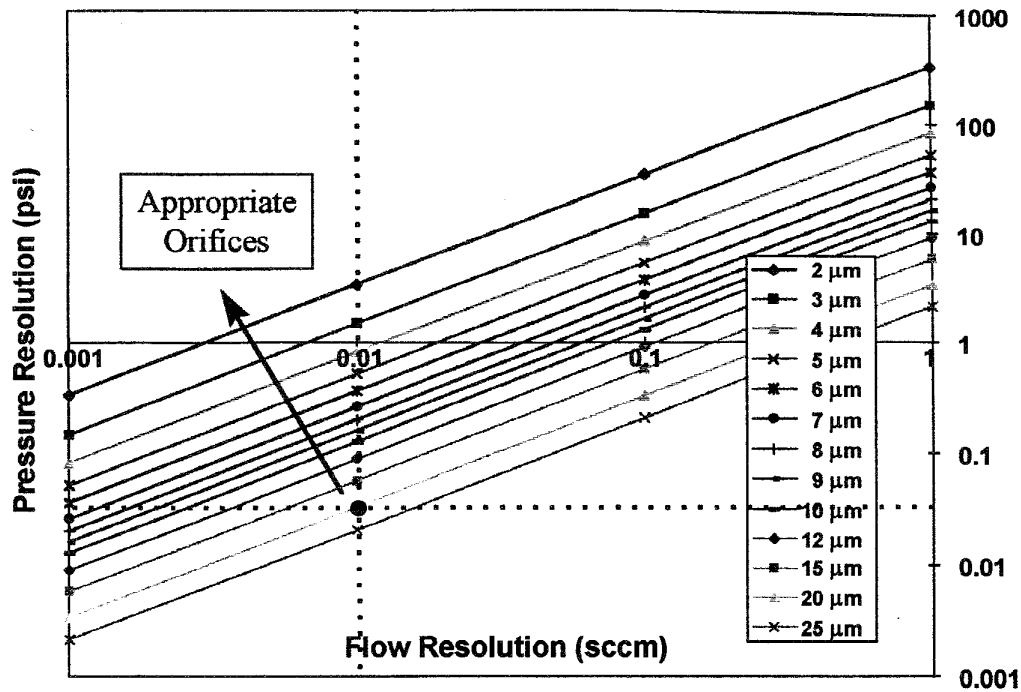
Figure 11: Pressure Sensor Resolution Required to Achieve a Given Flow Resolution, as a Function of Critical Orifice Hydraulic Diameter.

Flow Set Point

Electronics/ Control

P_{hi}

P_{sense}

P_{lo}

NO　　　**CO**
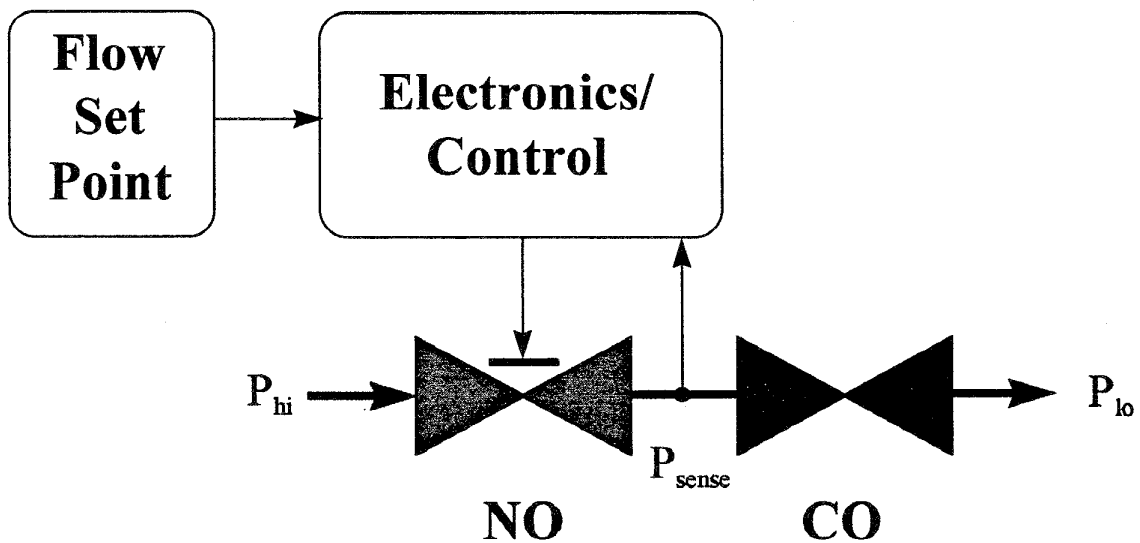
Figure 12: Schematic Representation of the Compressible Flow Model for the Series Combination of a Normally-Open Proportional Valve, and a Critical Orifice.
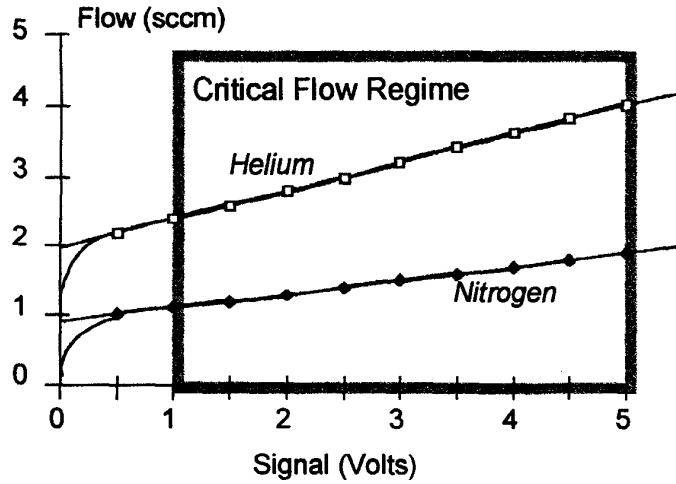
Figure 13: Measured Flow Characteristics for a Low-Flow MFC.
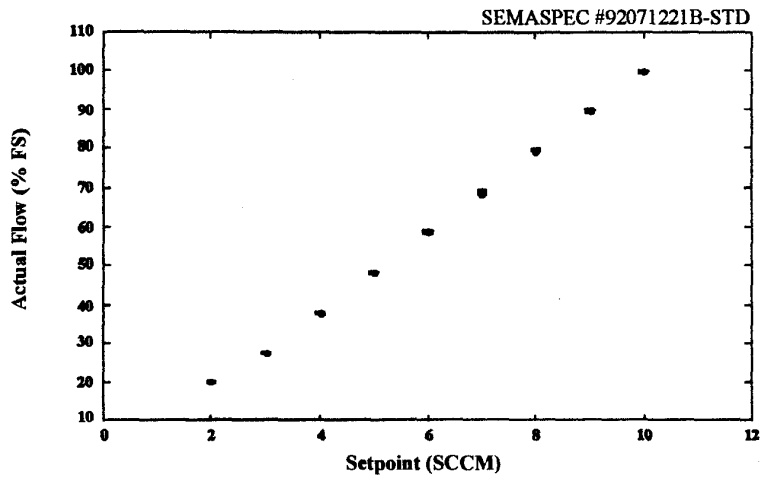
Figure 14: Measured Flow from a 10 sccm Mass-Flow Controller. The Measurements were Carried Out According to the SEMATECH Mass-Flow Controller Test Specification Shown.
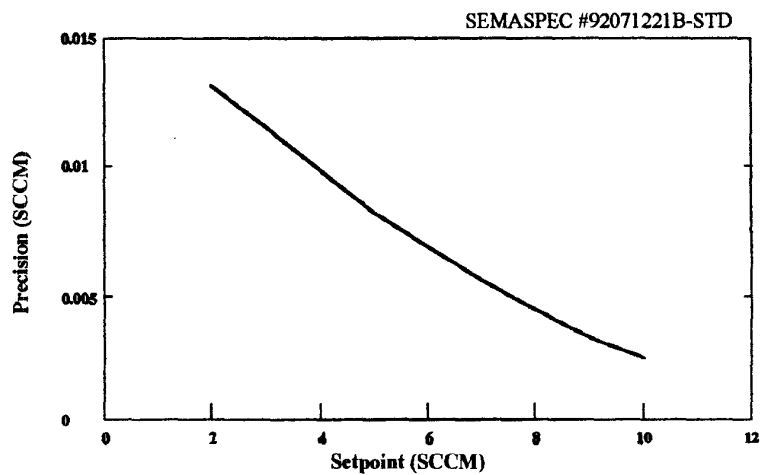
Figure 15: Measurement Precision Results from a 10 sccm Mass-Flow Controller.
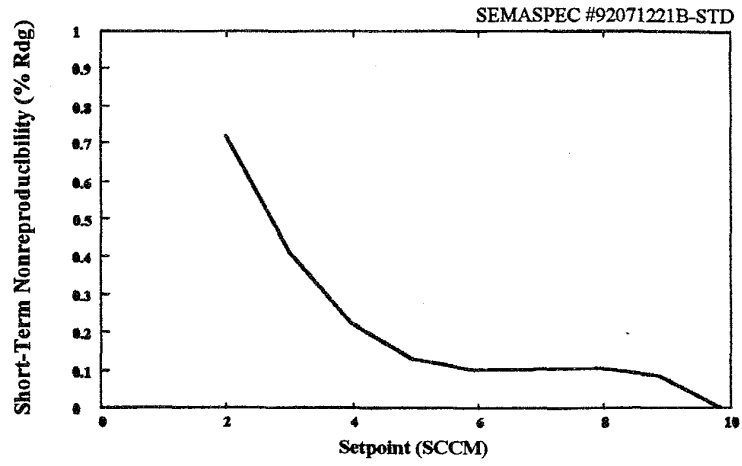
Figure 16: Measurement Reproducibility Results from a 10 sccm Mass-Flow Controller.
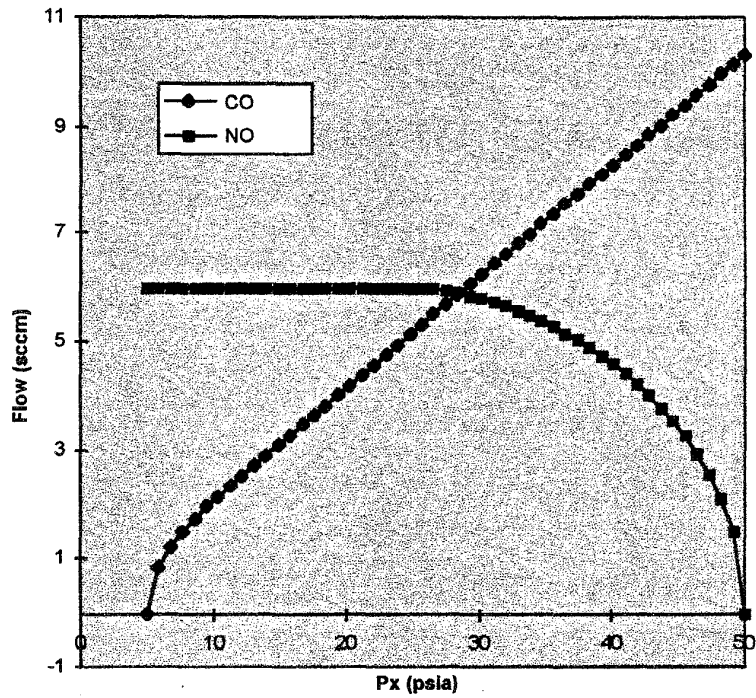
Figure 17: Flow Model for the MFC.

25 mm

29 mm
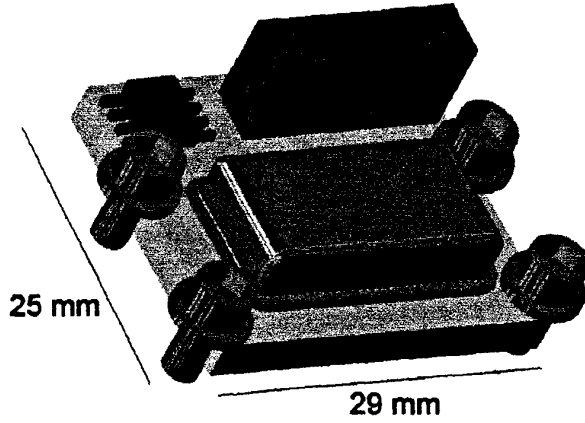
Figure 18: Example Isometric View of a Pressure Regulator, MFC, or Shut-Off Valve.

Shut-off   PR   Shut-off

1/8" VCR

Shut-off   MFC
(Purge)

140 mm

90 mm
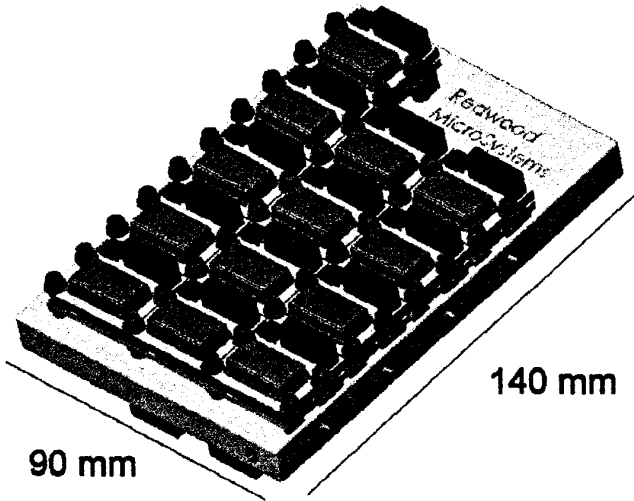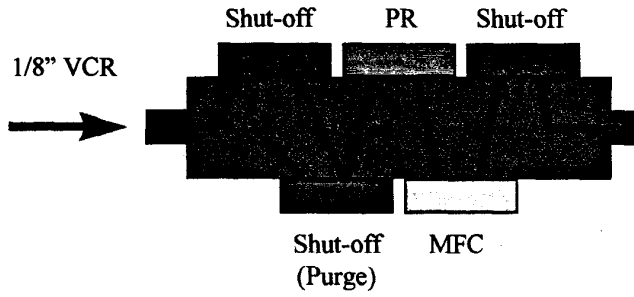
Figure 19: (upper) Schematic of One Channel of an Integrated Gas Stick; (lower) Isometric View of a
4-Channel Gas Stick.

S-O   PR   PT   S-O/Purge   MFC   S-O

Installed
Base*
1990
— 612 mm —

Face-Seal
MFC*
1995
— 545 mm —

Mono-Block
Design*
1996
— 326 mm —

Redwood
Phase 1
1997
156 mm

Redwood
Phase 2
1998
106 mm
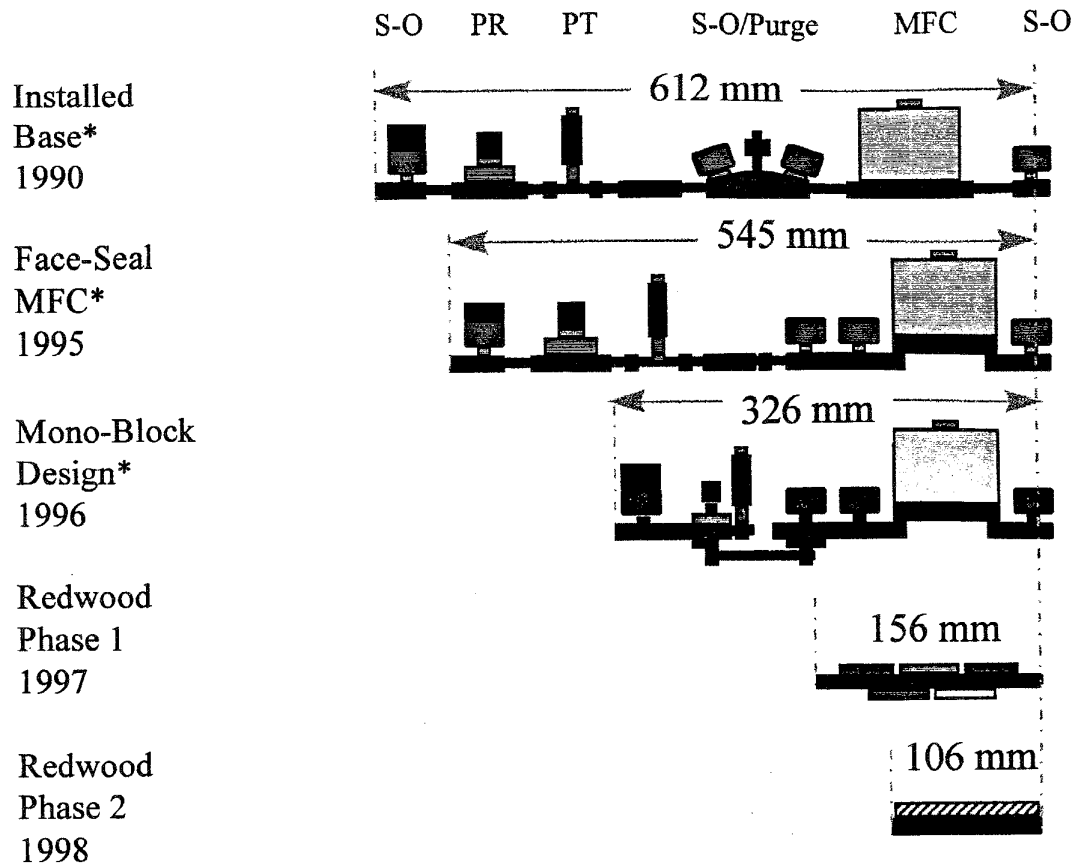
Figure 20: Size Comparison of Present and Future Integrated Gas Sticks/Panels (after [11]).